



# Study on the synthesis and photocatalysis of $\text{Ag}_3\text{PO}_4$ polyhedral microcrystals

TAO GENG<sup>1,2,\*</sup>, SHUANGBIN ZHANG<sup>1,2</sup> and YAO CHEN<sup>1</sup>

<sup>1</sup>School of Chemistry and Chemical Engineering, Suzhou University, Suzhou 234000, People's Republic of China

<sup>2</sup>Key Laboratory of Spin Electron and Nanomaterials of Anhui Higher Education Institute, Suzhou 234000, People's Republic of China

\*Author for correspondence (szxygt@163.com)

MS received 22 December 2019; accepted 11 March 2020

**Abstract.** The silver phosphate ( $\text{Ag}_3\text{PO}_4$ ) sample was synthesized using  $\text{Na}_3\text{PO}_4$ ,  $\text{AgNO}_3$  and PEG-10000 as raw materials by the hydrothermal method. Its different morphologies were obtained by changing temperature and surfactant. And its structures and morphology were characterized by X-ray diffraction and field emission scanning electron microscopy. The result of the study indicated that after the heat treatment at 150°C, the as-obtained  $\text{Ag}_3\text{PO}_4$  polyhedral microcrystal's diameter was about 4  $\mu\text{m}$ . Meanwhile, it showed that using  $\text{Ag}_3\text{PO}_4$  polyhedral microcrystals as photocatalysts, the photocatalytic degradation rate of methylene blue in aqueous solution was close to 98.5% after 25 min of sunlight.

**Keywords.** Photocatalysis;  $\text{Ag}_3\text{PO}_4$ ; hydrothermal method; methylene blue.

## 1. Introduction

With the rapid development of industrial production, the environmental pollution is getting worse and worse day by day. Especially the more and more organic pollutant in wastewater brought by the printing and dyeing industry makes our living environment increasingly deteriorating [1–4]. In fact, it is threatening our existence. Therefore, it will be of great significance to effectively deal with wastewater organic pollutant which is produced by the printing and dyeing industry, then impose on environmental protection and improve the quality of water circumstances [5]. Photocatalysis, as a green technology, aided by photocatalysts, is widely used to catalyse the degradation of organic pollutants under the light. Among semiconductor photocatalysts, the  $\text{Ag}_3\text{PO}_4$  sample is a hit subject due to its obvious advantage that it can absorb sunlight at wavelengths less than 520 nm and under the irradiation of light shows a strong oxidation capacity [6].  $\text{Ag}_3\text{PO}_4$  as a narrow band gap semiconductor, a visible light novel photocatalyst with an indirect band gap of 2.36 eV, under visible light irradiation, the electrons in the valence band (VB) of  $\text{Ag}_3\text{PO}_4$  were excited to conduction band (CB) to generate electron–hole pairs [7]. Furthermore, reactive holes at VB are able to oxidize organic dye pollutants directly to  $\text{CO}_2$  and  $\text{H}_2\text{O}$  because of its intense oxidation.

In 2010, Ye and his co-workers [8] discovered  $\text{Ag}_3\text{PO}_4$  as a new and meaningful photocatalyst, and furthermore found that it has extremely high efficiency for degradation organic

dyes in visible light irradiation. It is well known that the properties of nanomaterials are greatly affected by the morphology, structure and phase. The same is true for photocatalytic properties. For the sake of improving and optimizing the photocatalytic activity of  $\text{Ag}_3\text{PO}_4$ , researchers do a lot of work to further synthesize its different shape, and remarkable achievement has been made. So far,  $\text{Ag}_3\text{PO}_4$  photocatalysts with many distinction morphologies, including tetrahedron [9], hierarchical porous microtube [10], cube [11], nanosphere [7,12], dodecahedron [13], branch [14] and tetrapod [15] and further study will be continuing. Li *et al* [16] illustrated the principal mechanism for the excellent photocatalytic performance, summarized some common synthesis methods, discussed barriers and solutions for the practical application of  $\text{Ag}_3\text{PO}_4$ . David *et al* [17] explained the structure and properties of  $\text{Ag}_3\text{PO}_4$ . The authors recommend facet control and surface modification of  $\text{Ag}_3\text{PO}_4$  for water photo-oxidation and they elaborated photocatalytic performance in decomposition organic contaminants of using  $\text{Ag}_3\text{PO}_4$ . Xie *et al* [13] reported a simple combination craft for the prepared micron-structured  $\text{Ag}_3\text{PO}_4$  materials, which act as photocatalysts for photocatalytic degradation rhodamine B organic dye in visible light irradiation, achieve good photocatalytic effect. Besides, Xiong *et al* [18] reveals that using  $\text{Ag}_3\text{PO}_4$  and chitosan fibre composite nanomaterials as photocatalysts, the photocatalytic degradation rate can reach up to 93.8% in 80 min of visible light irradiation for degradation of methyl orange. Hence, plenty of researches

prove that the  $\text{Ag}_3\text{PO}_4$  sample has better visible light photocatalytic activity in photocatalytic degradation of aromatic organic dyes [15,19–21] than previous methods of preparing  $\text{Ag}_3\text{PO}_4$  polyhedral microcrystals. Yet, related studies on photocatalytic performances are not found much in the literature.

In this paper, we synthesized  $\text{Ag}_3\text{PO}_4$  polyhedral microcrystals by a simple and mild hydrothermal way, and then elaborated the photocatalytic degradation properties of  $\text{Ag}_3\text{PO}_4$  as photocatalysts for photocatalytic degradation of methylene blue (MB) in visible light irradiation.

## 2. Experimental

### 2.1 Synthesis of $\text{Ag}_3\text{PO}_4$ polyhedral microcrystals

In a typical experimental procedure, firstly, 0.34 g  $\text{AgNO}_3$  and 0.38 g  $\text{Na}_3\text{PO}_4$  were separately dissolved into 15 ml deionized water to become a uniform solution, and the solution was kept under vigorous magnetic stirring at room temperature for 10 min. Then, 0.5 g PEG-10000 was weighed and dissolved in 10 ml deionized water. Next, the 0.5 g PEG-10000 solution was introduced into  $\text{AgNO}_3$  solution and mixed. After continuously stirring at room temperature for another 10 min, 0.38 g  $\text{Na}_3\text{PO}_4$  solution was slowly added into  $\text{AgNO}_3$  solutions and vigorously magnetically stirred at room temperature for 10 min once more, making the three substances well mixed, then the mixed solution was poured into a 50 ml Teflon-lined stainless steel high-temperature reaction kettle and the kettle was heated at  $150^\circ\text{C}$  for 8 h. Finally, after the system was cooled to room temperature naturally, the products were collected, the precipitates were washed with distilled water and absolute ethyl alcohol three times, and they were dried in a vacuum at  $60^\circ\text{C}$  for 12 h. At last, we obtained  $\text{Ag}_3\text{PO}_4$  powder products.

We also obtained  $\text{Ag}_3\text{PO}_4$  powder products if the above experimental process was repeated under the same conditions except the reaction temperature was  $120$  or  $180^\circ\text{C}$ . In addition, powder products could be acquired as well under the same experimental conditions at  $150^\circ\text{C}$  for 8 h in the absence of surfactant PEG-10000.

### 2.2 Characterization

X-ray powder diffraction (XRD) of the products was carried out by the Dx-2600 model X-ray diffractometer of Liaoning Dandong Fangyuan Instrument Co. Ltd, at a scanning rate of  $0.1^\circ \text{s}^{-1}$  with  $2\theta$  ranging from  $20$  to  $80^\circ$ . A field emission scanning electron microscope (FESEM) was applied to observe the picture of the surface morphology of the materials by a Hitachi S-4800, at an accelerating voltage from  $5$  to  $15 \text{ kV}$ . Correspondingly, UV–visible absorption spectra were utilized to detect the change of absorbance of

degraded rhodamine B solution by the Hitachi U-3310 UV–visible absorption spectrophotometer (Japan).

### 2.3 Photocatalytic tests

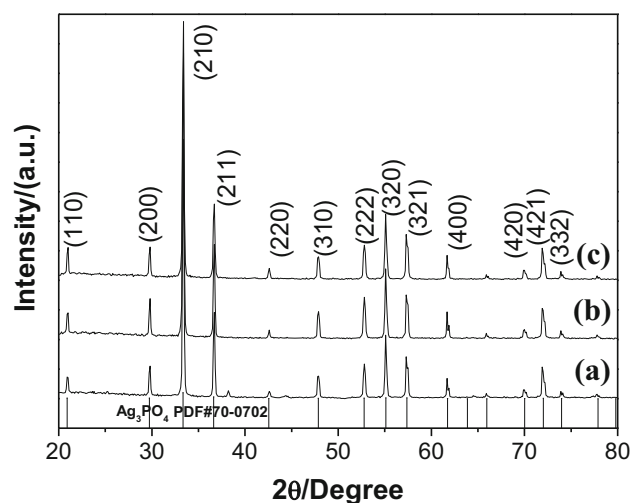
A total of  $0.01 \text{ g}$   $\text{Ag}_3\text{PO}_4$  product was weighed and added into  $50 \text{ ml}$  of  $10 \text{ mg l}^{-1}$  MB aqueous solution and was vigorously magnetically stirred for  $10 \text{ min}$  in the absence of light in order to achieve adsorption equilibrium. Then, we need to take samples in the mixed systems every  $5 \text{ min}$  in sunlight irradiation. After its centrifugation, the supernatant was selected and the change of the absorbance of degraded MB solution was detected by a U-3310 UV–visible spectrometer.

## 3. Results and discussion

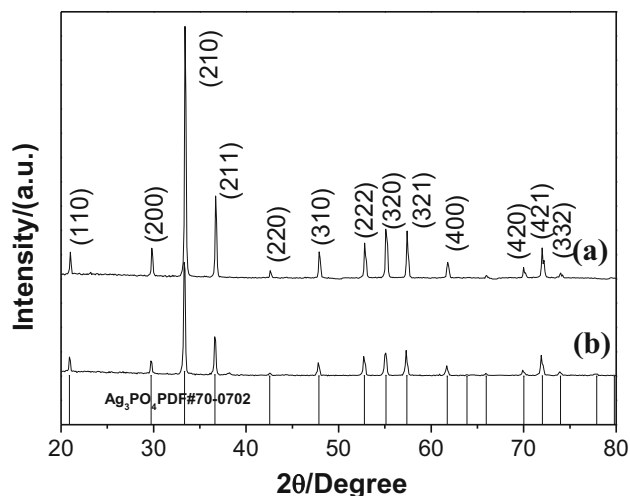
### 3.1 Structure and morphology analysis

Figure 1 depicts the XRD pattern of the as-obtained products under different reaction temperature conditions. As can be seen from the curves (a), (b) and (c), all typical diffraction peaks centred at  $2\theta$  as  $20.9$ ,  $29.7$ ,  $30.3$ ,  $36.6$ ,  $42.5$ ,  $47.8$ ,  $52.7$ ,  $55.1$ ,  $57.3$ ,  $61.7$ ,  $70.0$ ,  $71.9$  and  $73.9^\circ$  could be referenced to a polyhedral  $\text{Ag}_3\text{PO}_4$  product phase corresponding to the (110), (200), (210), (211), (220), (310), (222), (320), (321), (400), (420), (421) and (332)  $\text{Ag}_3\text{PO}_4$  JCPDS no. 70-0702, and no impurity peaks appeared. The as-obtained product is definitely a cubic  $\text{Ag}_3\text{PO}_4$  crystal structure. The peak and peak width of samples prepared at different reaction temperatures are not exactly the same, so it can be inferred that the sample size is not entirely alike.

Figure 2 is the XRD patterns of the  $\text{Ag}_3\text{PO}_4$  sample in the presence or absence of PEG-10000 at  $150^\circ\text{C}$  for 8 h, and it shows the diffraction peak positions are absolutely in



**Figure 1.** XRD patterns of the  $\text{Ag}_3\text{PO}_4$  sample at different temperatures: (a)  $120^\circ\text{C}$ , (b)  $150^\circ\text{C}$  and (c)  $180^\circ\text{C}$ .



**Figure 2.** XRD patterns of the  $\text{Ag}_3\text{PO}_4$  sample at the same reaction temperature and time: (a) with PEG and (b) without PEG.

accordance with JCPDS no. 70-0702, and no impurity peaks appeared. Therefore, it can prove that the as-prepared sample is a cubic  $\text{Ag}_3\text{PO}_4$  crystal structure.

Figure 3 shows that the morphology of hydrothermal products characterized with FESEM (figure 3a–c) is also not completely the same in different reaction temperature conditions of the as-obtained sample. Figure 3b is the SEM image of the as-prepared  $\text{Ag}_3\text{PO}_4$  sample at 150°C, we found that is the polyhedral structure, the morphology of the products is relatively uniform with the size of about 4  $\mu\text{m}$ . Figure 3a and c is the SEM image of as-obtained  $\text{Ag}_3\text{PO}_4$

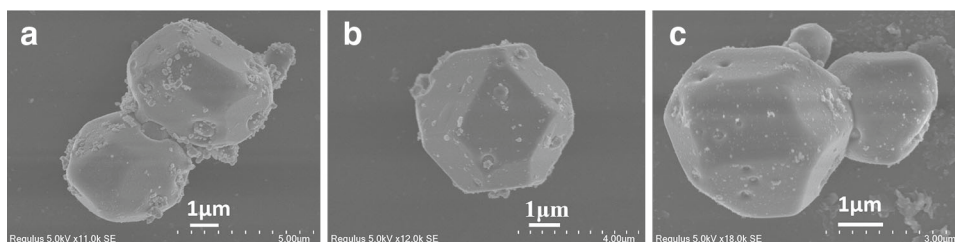
sample at 120 and 180°C. The structure is an irregular sphere or irregular polyhedron.

Figure 4a and b is the SEM image of the as-prepared  $\text{Ag}_3\text{PO}_4$  sample in the presence or absence of PEG-10000 which is in the same hydrothermal reaction temperature and time conditions. As it is shown, the morphology of the sample exhibits relatively neat and consistent polyhedral structure after added to the surfactant PEG-10000. Furthermore, the shape of the products is all stacked together, instead of uniform particle sizes and irregular ones due to the absence of PEG-10000.

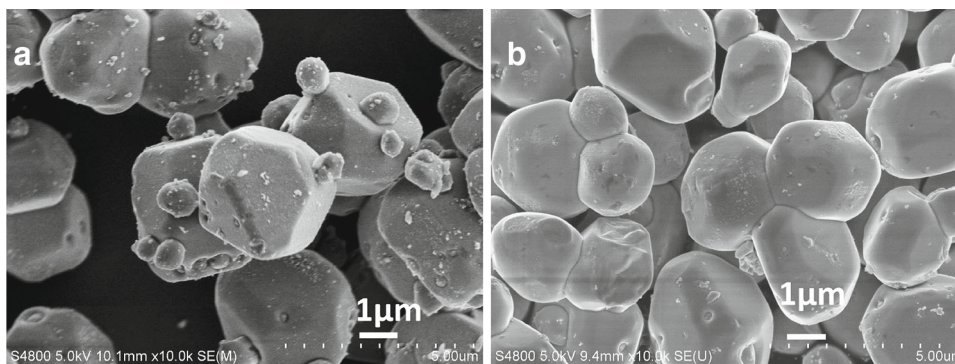
### 3.2 Photocatalytic performances

Figure 5 is the UV–visible absorption spectra of the as-obtained polyhedral microcrystal materials as photocatalysts by hydrothermal reaction at 150°C, which is a degraded MB by the different sunlight illumination times. As in figure 5, we can see that with the increase of visible light irradiation time, the max absorption peak of MB aqueous solution at 664 nm obviously decreases, and after 25 min of the visible light irradiation, the main absorption peak of MB water solution almost disappears. Moreover, the systems of the solution become colourless.

Figure 6a shows the change of the as-obtained  $\text{Ag}_3\text{PO}_4$  polyhedral microcrystal materials as photocatalyst in hydrothermal reaction 150°C for 8 h in the presence of PEG-10000 degradation curve, which is a degraded MB by different visible light illumination times. According to the degradation rate formula of degradation reaction:  $D\% = (C_0 - C)/C_0 \times 100\%$



**Figure 3.** SEM patterns of the  $\text{Ag}_3\text{PO}_4$  sample at different temperatures: (a) 120°C, (b) 150°C and (c) 180°C.



**Figure 4.** SEM patterns of the  $\text{Ag}_3\text{PO}_4$  sample: (a) with PEG and (b) without PEG.

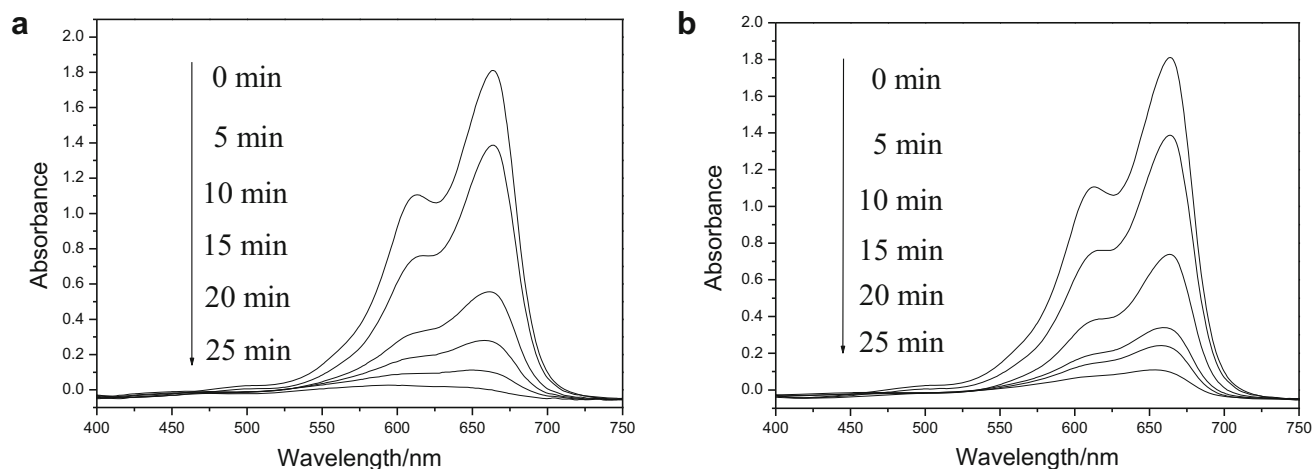


**Figure 5.** UV-visible absorption spectra of photocatalytic degradation for an aqueous solution of MB on  $\text{Ag}_3\text{PO}_4$  sample: (a) with PEG and (b) without PEG.

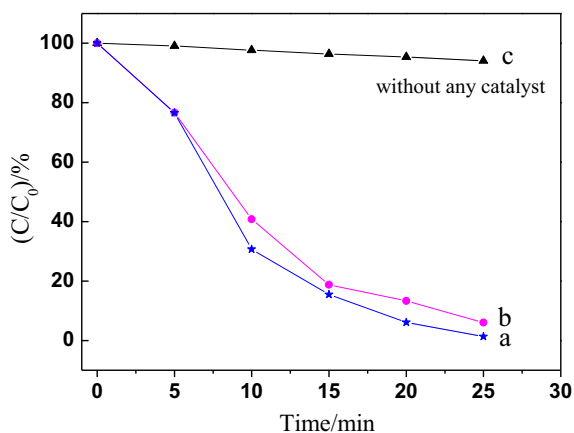


**Figure 6.** Photodegradation curves of MB: (a) with PEG and (b) without PEG.

[22,23], the degradation rate can reach 98.5% in 25 min visible light irradiation. Figure 6b shows that for as-synthesized  $\text{Ag}_3\text{PO}_4$  polyhedral microcrystals as photocatalyst in the same experimental conditions except for the absence of surfactant PEG-10000, after 25 min of the visible light irradiation, the degradation rate is 93.9%. Similarly, with none of photocatalyst, figure 6c shows that the degradation of MB is nearly invariant in the equal illumination time. So

we know that the  $\text{Ag}_3\text{PO}_4$  polyhedral microcrystals have outstanding photocatalytic activity for degraded MB aqueous solution, while the add PEG-10000 is superior to no PEG-10000 as a surfactant in the reaction system. We also compare some literature in photocatalytic degradation MB or other dyes (see table 1), the  $\text{Ag}_3\text{PO}_4$  polyhedral also presents better photocatalytic degradation ability than some  $\text{Ag}_3\text{PO}_4$  or  $\text{Ag}_3\text{PO}_4$  composite. The unique photocatalytic performance can be attributed to the  $\text{Ag}_3\text{PO}_4$  polyhedral shape which could effectively improve light harvesting. On the other hand, this polyhedral structure also could promote the separation of photo-excited carriers and decrease the probability of electron-hole recombination. Hence,  $\text{Ag}_3\text{PO}_4$  polyhedral nanospheres exhibit better photocatalytic performance.

#### 4. Conclusions

All in all, we have successfully prepared a uniform morphology with a size of about 4  $\mu\text{m}$  polyhedral  $\text{Ag}_3\text{PO}_4$  microcrystal structure through the hydrothermal route at 150°C for 8 h in the presence of the dispersing agent. More importantly, we have applied it as photocatalyst for the study on organic pollution dye MB photocatalytic

**Table 1.** The photocatalytic degradation rate of  $\text{Ag}_3\text{PO}_4$  for MB or other dyes in the foregoing literature.

Catalyst	Decolourization rates	Time (min)	References
$\text{Ag}_3\text{PO}_4$ polyhedral	98.5% (MB)	25	This work
$\text{Ag}_3\text{PO}_4/\text{CF}$	93.8% (methyl orange)	80	[18]
GQDs- $\text{Ag}_3\text{PO}_4$	94% (methyl orange)	25	[19]
$\text{Ag}_3\text{PO}_4$	67.14% (methyl orange)	25	[19]
$\text{Ag}_3\text{PO}_4$	Completely degrade (rhodamine B)	35	[21]
F-doped $\text{Ag}_3\text{PO}_4$	Completely degrade (rhodamine B)	15	[21]
$\text{Ag}_3\text{PO}_4$	77% (rhodamine B)	60	[24]

degradation experiment in visible light irradiation. And the experiment shows that the  $\text{Ag}_3\text{PO}_4$  sample has the excellent photocatalytic ability for degradation MB solution and attains a 98.5% degradation rate in the illumination time of 25 min.

### Acknowledgements

This work was financially supported by the Anhui Provincial Project of Outstanding Young Talents Fund in Universities (No. gxyqZD2016342); Suzhou University Professor Research Projects (No. 2017jb02); Innovative Research Team of Anhui Provincial Education Department (2016SCXPTTD) and Key Discipline of Material Science and Engineering of Suzhou University (2017XJZDXK3).

### References

- [1] Zhao G Y, Liu L J, Li J R and Liu Q 2016 *J. Alloys Compd.* **664** 169
- [2] Rupa A V, Manikandan D, Divakar D and Sivakumar T 2007 *J. Hazard. Mater.* **147** 906
- [3] Yang X F, Cui H Y, Li Y, Qin J L, Zhang R X and Tang H 2013 *ACS Catal.* **3** 363
- [4] Lv J L, Dai K, Lu L H, Geng L, Liang C H and Zhu G P 2016 *J. Alloys Compd.* **682** 778
- [5] Ge M, Zhu N, Zhao Y P, Li J and Liu L 2012 *Ind. Eng. Chem. Res.* **51** 5167
- [6] Tang C N, Liu E Z, Wan J, Hu X J and Fan J 2016 *Appl. Catal. B* **181** 707
- [7] Liu R D, Li H, Duan L B, Shen H, Zhang Q and Zhao X R 2018 *Appl. Surf. Sci.* **462** 263
- [8] Yi Z, Ye J, Kikugawa N, Kako T, Ouyang S, Stuart-Williams H *et al* 2010 *Nat. Mater.* **9** 559
- [9] Martin D J, Umezawa N, Chen X, Ye J and Tang J 2013 *Energy Environ. Sci.* **6** 3380
- [10] Liang Q, Ma W, Shi Y, Li Z and Yang X 2012 *Cryst EngComm* **14** 2966
- [11] Yang Z, Liu Y, Xu L, Huang G and Huang W 2014 *Mater. Lett.* **133** 139
- [12] Han C B, Li Y M, Wang W B, Hou Y J and Chen D F 2020 *Sci. Total Environ.* **704** 135356
- [13] Xie Y, Luo S Q, Huang H W, Huang Z H, Liu Y G, Fang M H *et al* 2018 *Colloids Surf. A* **546** 99
- [14] Dong P, Wang Y, Li H, Li H, Ma X and Han L 2013 *J. Mater. Chem. A* **1** 4651
- [15] Wang H, He L, Wang L H, Hu P F, Guo L, Han X D *et al* 2012 *CrystEngComm* **14** 8342
- [16] Li X P, Xu P, Chen M, Zeng G M, Wang D B, Chen F *et al* 2019 *Chem. Eng. J.* **366** 339
- [17] David J M, Liu G G, Moniz Savio J A, Bi Y P, Beale Andrew M, Ye J H *et al* 2015 *Chem. Soc. Rev.* **44** 7808
- [18] Xiong S W, Liu M, Yan J B, Zhao Z H, Wang H, Yin X Z *et al* 2018 *Cellulose* **25** 5007
- [19] Wang Y F, Wang H L, Xu A L and Song Z W 2018 *J. Mater. Sci.: Mater. Electron.* **29** 16691
- [20] Bi Y P, Hu H Y, Jiao Z B, Yu H C, Liu G X and Ye J H 2012 *Phys. Chem. Chem. Phys.* **14** 14486
- [21] Li S T, Shi S R, Huang G C, Xiong Y and Liu S W 2018 *Appl. Surf. Sci.* **455** 1139
- [22] Mohite S V, Ganbavle V V and Rajpure K Y 2016 *J. Alloys Compd.* **655** 106
- [23] Yang L and David F O 1996 *J. Catal.* **163** 1
- [24] Ma J L, Niu X J, Wang J and Wu J D 2016 *Catal. Commun.* **77** 55